Conference on Modelling Fluid Flow (CMFF'22)
The 18th International Conference on Fluid Flow Technologies
Budapest, Hungary, August 30-September 2, 2022

LES OF A NON-PREMIXED HYDROGEN FLAME STABILIZED BY WAVY-WALL BLUFF-BODY

Agnieszka WAWRZAK[1], Robert KANTOCH[2], Artur TYLISZCZAK[3]

[1] Department of Thermal Machinery, Faculty of Mechanical Engineering and Computer Science, Czestochowa University of Technology. Al. Armii Krajowej 21, 42-201 Czestochowa, Poland. Tel.: +48 34 3250 590, Fax: +48 34 3250 555, E-mail: agnieszka.wawrzak@pcz.pl
[2] Department of Thermal Machinery, Faculty of Mechanical Engineering and Computer Science, Czestochowa University of Technology. E-mail: robert.kantoch@pcz.pl
[3] Department of Thermal Machinery, Faculty of Mechanical Engineering and Computer Science, Czestochowa University of Technology. E-mail: artur.tyliszczak@pcz.pl

ABSTRACT

Numerical analysis of non-premixed hydrogen flames stabilized by specially designed bluff-bodies is presented. The response of the flame on the different wall topologies (flat or wavy, with the waviness oriented streamwise) is studied using large-eddy simulations (LES) and applying a two-stage procedure involving commercial ANSYS software and an in-house academic high-order code. The chemical source terms are calculated with the help of the 'no-model' approach. In addition, the study attempts to compare the obtained results with the solutions predicted by the Eulerian Stochastic Fields method. Dynamics of flames is found to be strongly dependent on geometrical shaping. In the case of the bluff-body with wavy walls the temperature isosurfaces reflect the bluff-body shape due to large-scale intense vortices induced in the outer shear-layer. The effect of change in wall topology is justified and quantified through time averaged mean and fluctuating quantities. It is the most pronounced in local entrainment of the fuel stream and flame radial position. When the waviness is applied to the bluff-body walls, the mixing is enhanced, the flame is noticeably shifted towards the axis and inlet plane, and slightly stretched in the radial direction compared to the flat wall. m

Keywords: bluff-body, Eulerian Fields, hydrogen, LES, non-premixed flames

NOMENCLATURE

D	$[mm]$	diameter
R	$[J/K\ mol]$	universal gas constant
T	$[K]$	temperature
U_b	$[m/s]$	bulk velocity of the co-flow
Y_α	$[-]$	species mass fractions
D_α	$[m^2/s]$	molecular diffusivity
h	$[J]$	enthalpy
p	$[Pa]$	hydrodynamic pressure
p_0	$[Pa]$	thermodynamic pressure
$\mathbf{S}$	[]	rate of strain tensor
$\boldsymbol{\tau}$	[]	stress tensor
$\mathbf{u}$	$[m/s]$	velocity vector
Δ	$[m]$	LES filter size
$\dot{\omega}_k$	$[mol/m^3\ s]$	reaction rate
μ	$[Pa\ s]$	molecular viscosity
ρ	$[kg/m^3]$	density
$\tilde{\phi}_\alpha$	$[-]$	reactive scalar
ξ^n_α	$[-]$	stochastic representation of the scalar

Subscripts and Superscripts

α	indices of the species
SGS, t	related to sub-grid or turbulent
t	time

1. INTRODUCTION

A better understanding of mutual interactions between turbulent flow and flame occurring downstream the bluff-body geometries limit the further progress in improvements in the efficiency and safety of various combustion applications (burners, chambers, engines). Moreover, a suitable control of turbulent flames dynamics is required for establishment of low-emissions devices according to current international regulations. Such a control can be achieved by applying passive and/or active flow control techniques.Both provide modulation of the multi-scale mixing processes (enhancement/suppression) by the intensification of interactions between large and small turbulent scales.

Using the bluff-body as a part of the injection system constitutes the prominent example of the passive flame control. The bluff-body generates recirculation zones improving the mixing and stabilizing the flame position [1]. Tyliszczak et al. [2] examined a non-premixed flame stabilized in a central recirculation zone produced by a conical/cylindrical bluff-body. They showed that the flame is approach-

ing extinction due to even small changes in simulation parameters. Combination of the passive and active control methods can be applied for optimization of the combustion process in bluff-body burner as it was shown by Kypraiou et al. [3]. The researchers performed the experimental studies on the premixed, partially-premixed and non-premixed methane flames showing that the impact of acoustic oscillations on the bluff-body flames is directly related to the fuel injection system.

The complexity of turbulent mixing and combustion processes raises many important questions that still remain unanswered, despite the great interest of the scientific community in this field. For instance, to what extend does the mixing of the fuel and oxidizer downstream the bluff-body depend on the shape and roughness of the bluff-body? As it was recently demonstrated by [4], the wavy wall, with carefully selected waviness parameters, can effectively enhance the effect of amplitude modulation and hence increase wall shear stress and postpone turbulent separation.

The present paper aims at numerical simulations of non-premixed hydrogen flame stabilized by specially designed bluff-bodies with corrugated surfaces. Computational fluid dynamics (CFD) tools have been widely used for the flame control analyses providing the results related to the global characteristics and deep insight into flame structure and dynamics. In this work we use the Large Eddy Simulation approach and the 'no model' approach where the chemical sources terms are calculated directly from the Arrhenius formula using the filtered variables [5]. The response of the flame on different wall topologies (flat or wavy, with the waviness oriented streamwise) is thoroughly discussed based on instantaneous and time averaged results. For the selected cases we performed the calculations using the Eulerian Stochastic Fields (ESF) method [6] which in the past proved to be able to correctly capture the dynamics of turbulent flames [7, 8] and strongly non-stationary events like the blow-off of bluff-body flames [9]. Results obtained from these computations will be compared with predictions of 'no model' calculations to demonstrate that the sub-grid physics ignored by the no-model approach does not have significant impact on the results and presented during the conference.

2. MODELLING

2.1. LES Approach

In the present study we use two different numerical LES solvers applying two-stage approach. In the first stage, the second order ANSYS Fluent LES solver is involved to model the flow inside the inlet section of the bluff-body burner. The further calculations are performed using a in-house high-order numerical algorithm based on the projection methods[10]. It solves the Favre filtered set of the governing equations assuming the low Mach number approximation [11]:

$$\partial_t \bar{\rho} + \nabla \cdot (\bar{\rho}\widetilde{\mathbf{u}}) = 0 \tag{1}$$

$$\bar{\rho}\partial_t \widetilde{\mathbf{u}} + (\bar{\rho}\widetilde{\mathbf{u}} \cdot \nabla)\widetilde{\mathbf{u}} + \nabla \bar{p} = \nabla \cdot \left(\boldsymbol{\tau} + \boldsymbol{\tau}^{\mathrm{SGS}}\right) \tag{2}$$

$$\bar{\rho}\partial_t \widetilde{Y}_\alpha + (\bar{\rho}\widetilde{\mathbf{u}} \cdot \nabla)\widetilde{Y}_\alpha = \nabla \cdot \left(\bar{\rho}(D_\alpha + D_\alpha^{\mathrm{SGS}})\nabla \widetilde{Y}_\alpha\right) + \overline{\dot{w}}_\alpha \tag{3}$$

$$\bar{\rho}\partial_t \widetilde{h} + (\bar{\rho}\widetilde{\mathbf{u}} \cdot \nabla)\widetilde{h} = \nabla \cdot \left(\bar{\rho}(D + D^{\mathrm{SGS}})\nabla h\right) \tag{4}$$

$$p_0 = \overline{\rho} R \widetilde{T} \tag{5}$$

where the bar and tilde symbols denote filtered quantities, u_i are the velocity components, p is the hydrodynamic pressure, ρ is the density and h stands for the total enthalpy. The symbols p_0 and R are the thermodynamic pressure and gas constant, respectively. The subscript α is the index of the species $\alpha = 1, \ldots,$ N-species whereas the variables Y_α represent species mass fractions. An unresolved sub-grid stress tensor, resulting from the filtering of the non-linear advection terms is defined as $\boldsymbol{\tau}^{\mathrm{SGS}} = 2\mu_{\mathrm{t}}\mathbf{S}$, where $\mathbf{S}$ is the rate of strain tensor of the resolved velocity field and μ_{t} is the sub-grid viscosity computed according to the model proposed by Vreman [12]. The sub-grid diffusivities in Eqs. 3, 4 are computed as $D^{\mathrm{SGS}} = \mu_t/(\bar{\rho}\sigma)$ where σ is the turbulent Schmidt/Prandtl number assumed equal to 0.7 [7].

The chemical sources terms $\overline{\dot{w}_\alpha}$ in Eq. 3 involve the filtered reaction rates of species α, which are strongly non-linear functions of the species mass fractions and enthalpy:

$$\overline{\dot{w}_\alpha(\mathbf{Y}, h)} = \dot{w}_\alpha(\widetilde{\mathbf{Y}}, \widetilde{h}) + \mathcal{F}(\widetilde{Y_\alpha Y_\alpha}'', \widetilde{Y_\alpha}''\widetilde{T}, \ldots) \tag{6}$$

They are computed applying the 'no model' approach, i.e., they are calculated directly from the Arrhenius formula using the filtered variable $\overline{\dot{w}_\alpha(\mathbf{Y}, h)} = \dot{w}_\alpha(\widetilde{\mathbf{Y}}, \widetilde{h})$ [5] or eigth or four ESF [6]. In the ESF combustion model the scalar Equations (3) and (4) are replaced by an equivalent evolution equation for the density-weighted filtered PDF function, which is solved using the stochastic field method proposed by Valiño [6]. Each scalar $\tilde{\phi}_\alpha$ is represented by $1 \le n \le N_s$ stochastic fields ξ_α^n such that

$$\tilde{\phi}_\alpha = \frac{1}{N_s}\sum_{n=1}^{N_s} \xi_\alpha^n \tag{7}$$

The stochastic fields evolve according to:

$$\begin{aligned} \mathrm{d}\xi_\alpha^n = &- \widetilde{\mathbf{u}} \cdot \nabla \xi_\alpha^n \mathrm{d}t + \nabla \cdot \left(\left(D_\alpha + D_\alpha^{SGS}\right) \nabla \xi_\alpha^n\right) \mathrm{d}t \\ &+ \sqrt{2 D_\alpha^{SGS}}\, \nabla \xi_\alpha^n \cdot \mathrm{d}\mathbf{W} - 0.5\tau^{-1}\left(\xi_\alpha^n - \tilde{\phi}_\alpha\right)\mathrm{d}t \\ &+ \dot{w}_\alpha(\xi_\alpha^n)\mathrm{d}t \end{aligned}$$

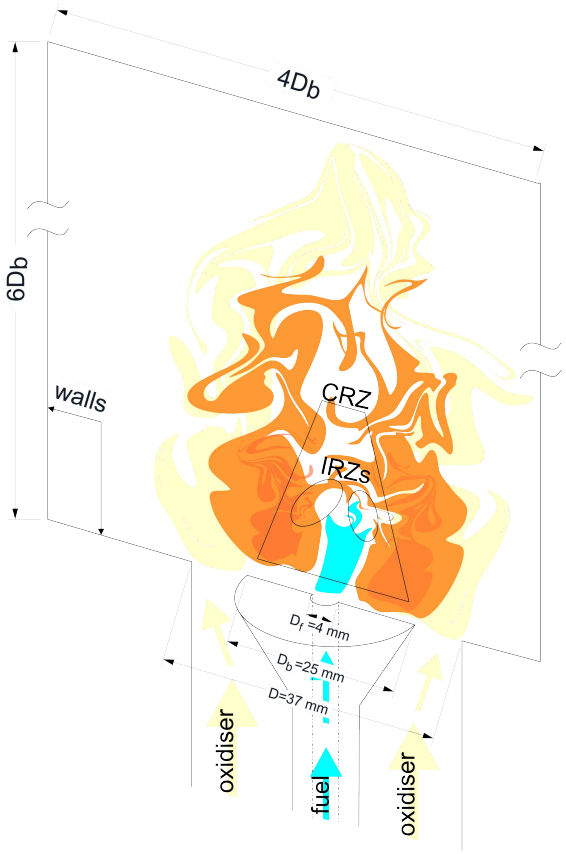

Figure 1. Schematic view on the computational configuration.

(8)

where the micro-mixing time scale equals to $\tau = \bar{\rho}\Delta^2/(\mu + \mu_t)$ [7] with $\Delta = V_{\text{cell}}^{1/3}$ being the LES filter width and d**W** represents a vector of Wiener process increments different for each field. The impact of the modelling of the chemical source terms will be discussed during the conference. In this paper we limit to the cases simulated using the 'no model' approach.

2.2. Test case

In the present work we consider a typical combustion chamber with the conical bluff-body similar to the one studied experimentally by Kypraiou et al. [3] but instead of methane, we use the hydrogen diluted with nitrogen, which is an alternative zero-carbon fuel. The hydrogen mass fraction in the fuel stream is equal to 0.05. Schematic view on the problem considered is presented in Figure 1. The cold (300 K) fuel is injected to the chamber through the 4mm slot in a fuel pipe ended with a bluff-body with the axial velocity assumed equal to 10 m/s. Inside the chamber the fuel ignites in hot (1000 K) co-flowing air. The combustion power is 0.5 kW and the equivalence ratio is equal to 0.047. Unlike in the original configuration of Kypraiou et al. [3] we do not add the swirl to the oxidiser stream and the dominant effect on the flame is due to the changing geometry of the

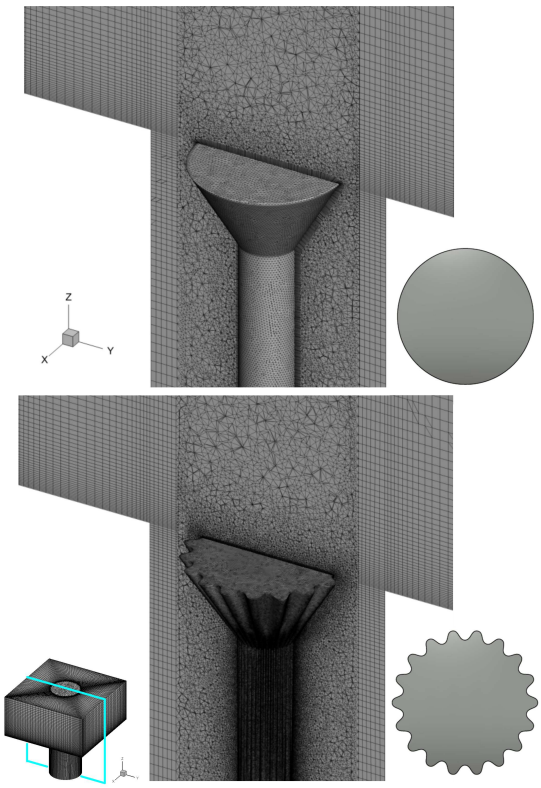

Figure 2. Bluff-body geometries and computational meshes (ANSYS Meshing).

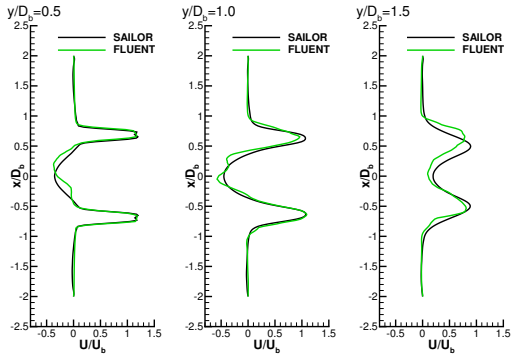

Figure 3. Axial velocity profiles at three different heights above the bluff-body obtained using Fluent and SAILOR codes.

bluff-body. Thus, a comparison with experimental results, even qualitative, is impossible.

Concerning the dynamics of the bluff-body stabilized flames, directly above the bluff-body a central recirculation zone (CRZ in Fig. 1) is formed. Its dimensions and inner structure depend on the bluff-body size and flow parameters. Inside CRZ may exist smaller inner recirculation zones (IRZs). The bluff-bodies investigated in the paper are characterised by the equivalent diameter $D_b = 2\sqrt{S/\pi}$=25 mm (S - actual area of bluff body) and they are placed in a circular duct of diameter D=37 mm. Two different

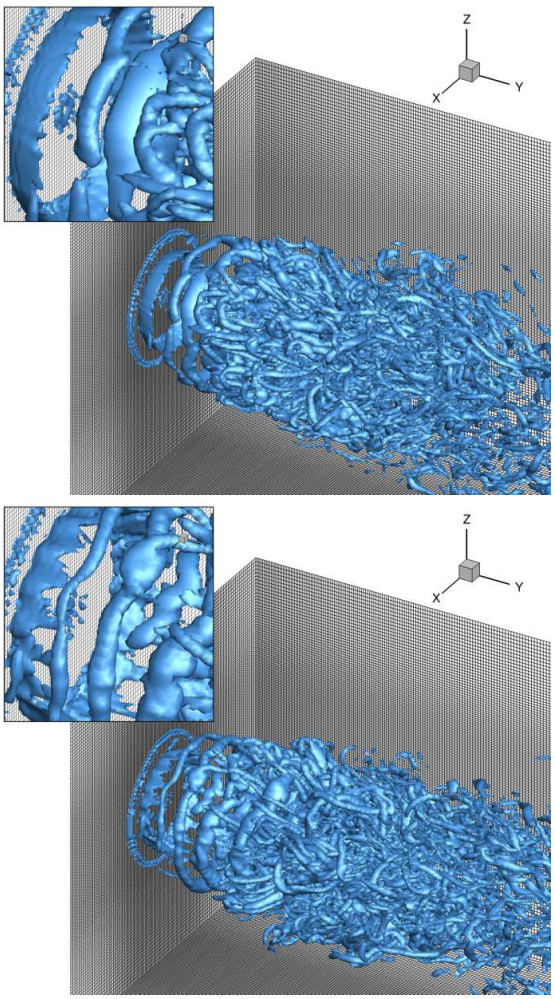

Figure 4. Visualization of the vortex structures. Instantaneous Q-parameter isosurfaces for bluff-bodies with different wall topologies (flat wall - upper row, wavy wall - bottom row). Computational mesh (SAILOR).

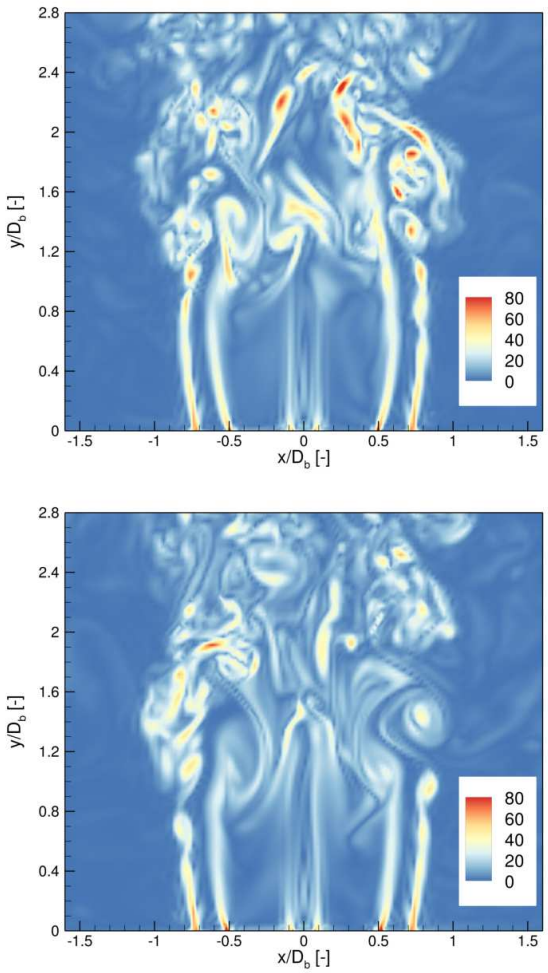

Figure 5. Instantaneous vorticity contours (flat wall - upper row, wavy wall - bottom row).

bluff-bodies are considered, with flat and wavy wall with the waviness oriented streamwise. Both geometries are displayed in Figure 2 along with the computational meshes prepared in the ANSYS Meshing module.

2.3. Numerical details

As mentioned before, the simulations are performed using a two-stage approach. In the first stage we involve the ANSYS Fluent LES solver to model flow through the entrance duct and around the bluff-bodies. In these preliminary calculations we acquire unsteady velocity signals at the end of the inlet section for a period of $150D_b/U_b$ (U_b- bulk velocity of the co-flow). In Fig. 2 the computational grids are presented generated in ANSYS Meshing module. They are block-structured and precisely fitted to the shape of each bluff-body. All geometries are discretized in this way that a near-wall cell height allows for a proper resolution of the turbulent boundary layers ($y+ \approx 1$). The minimum element size is assumed at the level of 0.5 mm for the case with flat wall, whereas in the case of the wavy-wall bluff-body a finer mesh (0.25 mm) in the near-wall region is needed. The overall numbers of cells in the inlet duct are equal to 3.6×10^5 and 3.7×10^5 for the cylindrical bluff-body with the smooth and wavy wall, respectively.

In the second part of the calculations a numerical code SAILOR [10], based on a high-order compact difference algorithm for low Mach number reactive flows, is used to predict the combustion process. Number of studies devoted to number of combustion problems in jet type flames [13, 14] and mixing layers [15, 16] verified the SAILOR codes confirming its accuracy. The extracted velocity fields are imposed onto the inlet plane of the computational domain involving only the outer section of the burner. The computational domain extends $6D_b$ in the axial direction and $4D_b$ in the radial and tangential directions (see Fig. 1). Grid independent solution is obtained at a grid size $N_x \times N_z \times N_y = 144 \times 144 \times 192$ nodes. The nodes are compacted axially and ra-

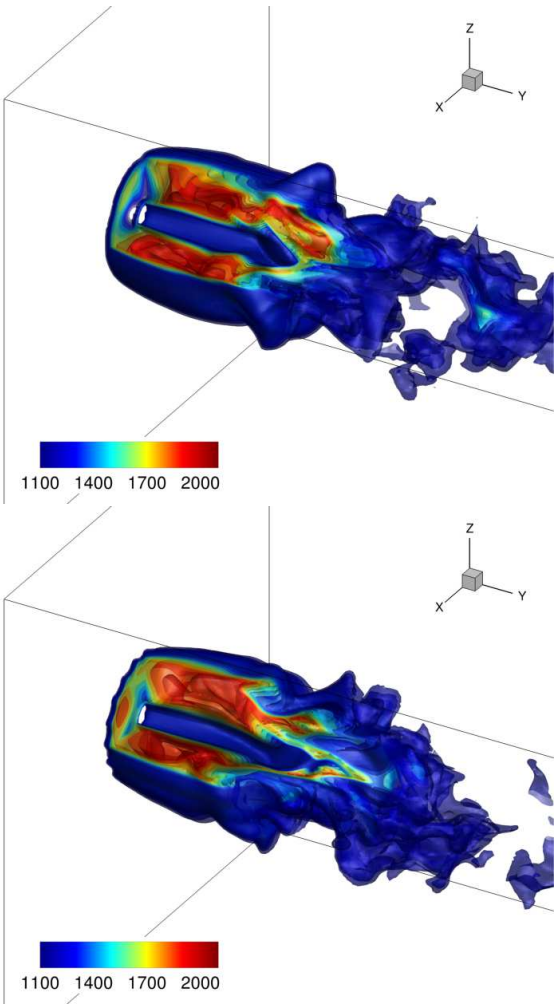

Figure 6. Visualization of flames stabilised by bluff-bodies with different wall topologies (flat wall - upper row, wavy wall - bottom row). Instantaneous temperature isosurfaces.

dially such that almost a uniform grid nodes distribution is ensured at the inlet section (see Figure 4. Maximum cell volume is equal to 1.7×10^{-9} m^3, that corresponds to the minimum cell volume of the computational meshes used in ANSYS software. The time-step is computed according to the Courant-Friedrichs-Lewy (CFL) condition with the maximum CFL number equal to 0.25. Concerning the boundary conditions at the side boundaries, the velocity is set to zero and the species and enthalpy are computed form the Neumann condition, i.e., $\partial Y_\alpha/\partial n = 0$ and $\partial h/\partial n = 0$. The pressure is computed from the Neumann condition ($\partial p/\partial n = 0$) both at the side boundaries as well as at the inlet plane. At the outlet boundary, all velocity components, species and enthalpy are computed from the convective boundary condition $\partial C/\partial t + V_c \partial C/\partial y = 0$, where C represents a general variable and V_c is the calculated as the mean velocity in the outlet plane. To avoid back-flow the velocity V_c is limited such that $V_c = \max(V_c, 0)$. The pressure at the outflow is assumed constant $p = 101325$ Pa.

The SAILOR code uses the projection method for pressure-velocity coupling [10] combined with a predictor-corrector method (Adams-Bashforth / Adams-Moulton) applied for the time integration. The spatial discretization is performed on half-staggered meshes by the 6th order compact finite difference approximation for the momentum and continuity equations. The second-order TVD (Total Variation Diminishing) scheme with Koren limiter is used for the transport equations for chemical species and enthalpy. The time integration of the chemical source is performed with the help of the VODPK (Variable-coefficient Ordinary Differential equation solver with the Preconditioned Krylov method) solver [17] that is well suited for stiff systems. The chemical reaction terms are computed using the CHEMKIN interpreter. The chemical reactions are computed using detailed mechanism of Mueller et al. [18] involving 9 species and 21 reactions for the hydrogen oxidation.

Preliminary simulations performed using ANSYS Fluent and the SAILOR code for the air stream flowing in the duct around the cylindrical bluff-body were conducted to verify the solution strategy. The comparison of the velocity profiles behind the bluff-body revealed that an interpolation of the velocity components related to two-stage procedure does not introduce significant errors. As can be seen in Fig. 3 both solvers provided similar velocity evolution downstream of the bluff-body. However, the results obtained using the SAILOR code seem to be more accurate, at least qualitatively, as they reflect the symmetric shape of the bluff-body. Furthermore, the applied two-stage approach was proven to yield correct results in previous studies devoted to passively controlled jet flames issuing from polygonal nozzles [19].

3. RESULTS

As the streams of fuel and oxidiser are ejected from the inlet plane into quiescent surroundings, the flow undergoes a Kelvin-Helmholtz instability due to a velocity gradient. The vortex rings are generated and detached from the shear layer generated near the bluff body edge. Their shape is respective to the bluff-body shape and in case of the wavy wall the wavy shaped rings are generated. This can be verified from Q-parameter isosurfaces presented in Fig. 4. Since the initial vortices are considerably different when the wall topology varies, their distortion changes as they travel in the downstream direction. An earlier formation of streamwise structures is seen for the flat wall, whereas stronger vortex rings in case of the wavy wall are observed further downstream revealing more complex flow structure. This can be further verified with the help of the vorticity magnitude plotted on the central cross-section and presented in Figure 5. Comparison of the vorticity contours reveals that flow inside CRZ is more intense

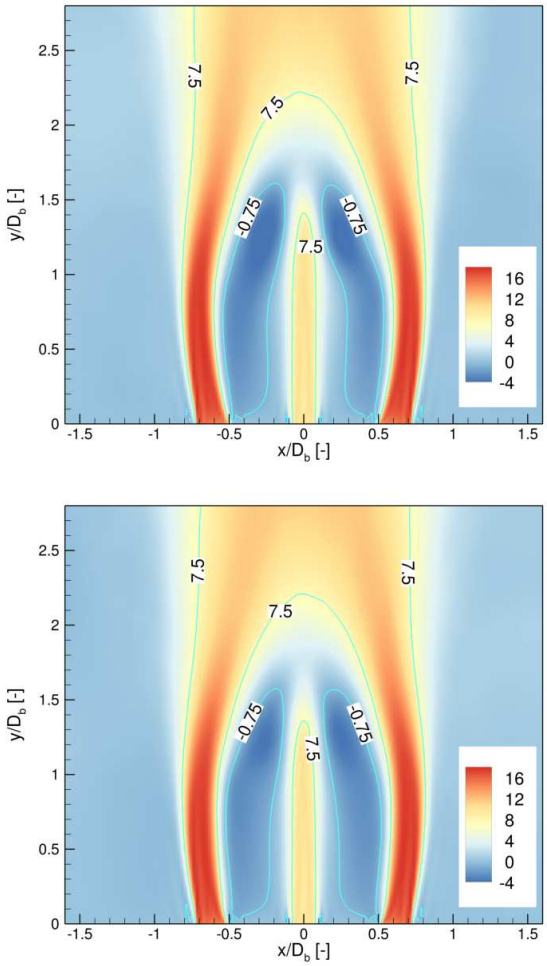

Figure 7. Time averaged axial velocity (mean) contours and isolines (flat wall - upper row, wavy wall - bottom row).

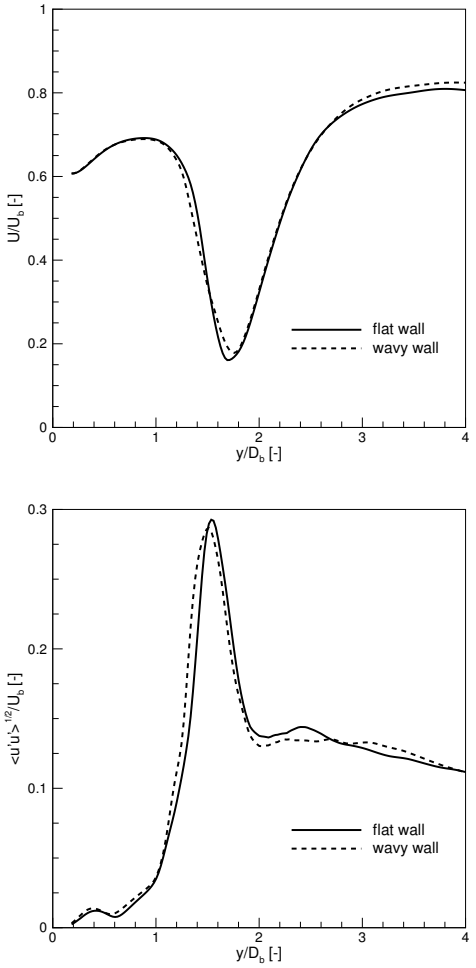

Figure 8. Time averaged axial velocity (mean and rms) along the centreline.

for the case with the wavy wall. With complex wall topology, isolevels seem more wrinkled in an earlier axial location. Similar observation can also be made by comparing isosurfaces of temperature in Figure 6 visualizing topology of the flame. Moreover, the flames reflect the shapes of the bluff-bodies attaching the inlet plane. Therefore, the effect of large-scale intense vortices induced in the outer shear-layer is prominent on the flame structure and shape.

Detailed analysis of the flame dynamics in central recirculation zone has been carried out based on time averaged results presented in Figures 7-10. The time-averaged procedure have been started after the flames had fully developed and continued for $250D_b/U_b$ resulting in fully convergent statistics. Form Fig. 7 it is evident that location of the recirculation zone is only slightly affected by the bluff-bodies geometries compared to the CRZ size and shape. The isoline of negative axial velocity in the case with wavy wall bluff-body is nearly parallel to the fuel stream contrary to the case with flat walls. It results in enhanced mixing manifested by more uniform velocity field inside CRZ. It is also visible in Fig. 7 that the fuel stream velocity decay earlier downstream in case of wavy wall. This confirms the fuel entrainment and enhancement of the fuel/oxidiser mixing. The reduction of the axial velocity along the centreline due to the application of the wavy wall is affected by the earlier growth of the fluctuations as presented in Figure 8. The local entrainment of the fuel stream can be deduced from the radial distribution of the mean hydrogen mass fraction at different distances behind the bluff-body presented in figure 9. The obtained profiles demonstrate the enhancement of the mixing for the case with wavy wall compared to the flat wall. It is manifested by reduced fuel mass fraction already behind the bluff-body (one diameter from the inlet).

In order to examine the impact of the wavy wall of the bluff-body on the flame structure the time-averaged temperature is compared along the radial direction at various axial distances in Figure 10. Increased ($\approx$ 45K) temperature is found at the axis and y/D_b=1.5, i.e, in the region where the recirculation

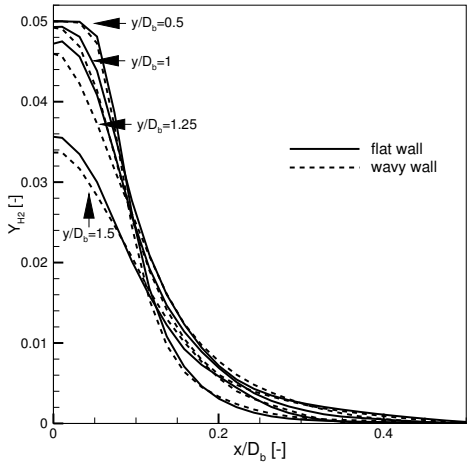

Figure 9. Radial distribution of the time averaged hydrogen mass fraction (mean) at different axial locations.

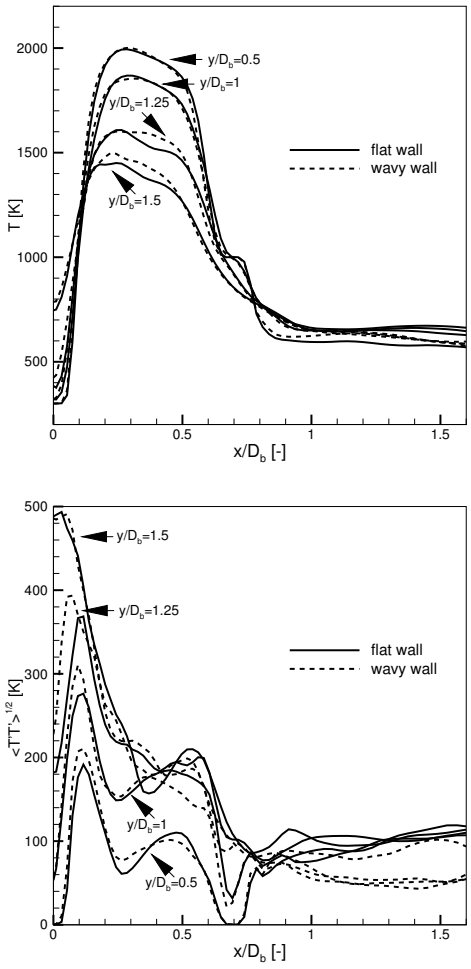

Figure 10. Radial profiles of the time averaged temperature (mean and rms) at different axial locations.

zone ends. This means that the flame appears further upstream compared to case with the flat wall. The increasing of the temperature for wavy wall is also observed in further radial locations respectively for various axial distances. The temperature is 40 K higher compared to the flat wall for radial distance x/D_b=0.1-0.2 and close the inlet plane (y/D_b=0.5-1) and 60 K higher at x/D_b=0.2-0.5 further downstream (y/D_b=1-1.25). Apparently, when the waviness is applied to the bluff-body walls, the flame is noticeably shifted towards the axis and the inlet plane. This is in line with the observation made for the velocity field and CRZ structure. Moreover, the flame is slightly stretched in the radial direction compared to the flat wall. However, the overall flame width does not change. Even more pronounced differences in the flame position are observed in axial distribution of the fluctuating component. One can observed in Fig. 10 that local maximum of the temperature fluctuations persists at x/Db=1 up to y/D_b=1 and shifts $0.05D_b$ towards axis at y/D_b=1.25 when the wavy wall is considered. Moreover, the contribution of the fluctuating component is considerably higher close the inlet plane and is transferred further downstream with 90 K higher values than for the flat wall. Such increase in the fluctuating quantities consistently affects the mean component.

4. SUMMARY

LES simulations of the bluff-body stabilized hydrogen non-premixed flame were carried out. The impact of wall topology (flat or wavy, with the waviness oriented streamwise) on the flame structure was studied for conventional bluff-body burner configuration with the help of second order LES solver provided by ANSYS and an in-house academic high-order code SAILOR. The solution procedure involved the generation of the set of the velocity profiles at the tip of bluff-body by simulating only the inlet section and simulations of the flames performed with the help of the acquired inlet velocity profiles. The chemical source terms were calculated with the help of the 'no-model' approach and comparison the obtained results with the Eulerian Stochatic Fields method will be presented during the conference.

The effect of geometrical shaping was manifested by the flame surfaces reflecting the strong vortex induced in the outer shear-layer which in turn were effectively shaped by wavy walls. Application of the wavy walls enhanced the mixing processes in CRZ comparing to the conventional flat walls. The impact of change in wall topology observed in instantaneous results were justified and quantified with the help of time averaged plots of mean and fluctuating velocity and temperature. The time averaged velocity distributions revealed the fuel entrainment earlier downstream and enhancement of the fuel/oxidiser mixing for the wavy walls applied. Moreover, the time averaged temperature was noticeably higher inside the central recirculation zone at x/D_b=0.2-0.5

and y/D_b=1-1.25 whereas the local maximum of the temperature fluctuations was shifted towards axis when the wall topology was changed. These observations allow to deduce that in case of wavy wall the fuel stream is earlier entranced and flame is shifted towards the centreline.

ACKNOWLEDGEMENTS

This work was supported by the National Science Center in Poland (Grant 2020/39/B/ST8/02802) and statutory founds (BS/PB-1-100-3011/2022/P). The computations were carried out using the PL-Grid Infrastructure.

REFERENCES

[1] Docquier, N., and Candel, S., 2002, "Combustion control and sensors: a review", *Prog Energy Combust Sci*, Vol. 28 (2), pp. 107–150.

[2] Tyliszczak, A., Cavaliere, D., and Mastorakos, E., 2014, "LES/CMC of blow-off in a liquid fueled swirl burner", *Flow Turbul Combust*, Vol. 92 (1-2), pp. 237–267.

[3] Kypraiou, A., Allison, P., Giusti, A., and Mastorakos, E., 2018, "Response of flames with different degrees of premixedness to acoustic oscillations", *Combust Sci Technol*, Vol. 190 (8), pp. 1426–1441.

[4] Dróżdż, A., Niegodajew, P., Romańczyk, M., Sokolenko, V., and Elsner, W., 2021, "Effective use of the streamwise waviness in the control of turbulent separation", *Exp Therm Fluid Sci*, Vol. 121, p. 110291.

[5] Duwig, C., Nogenmyr, K.-J., Chan, C.-k., and Dunn, M. J., 2011, "Large Eddy Simulations of a piloted lean premix jet flame using finite-rate chemistry", *Combust Theory Model*, Vol. 15 (4), pp. 537–568.

[6] Valino, L., Mustata, R., and Letaief, K. B., 2016, "Consistent behavior of Eulerian Monte Carlo fields at low Reynolds numbers", *Flow Turbul Combust*, Vol. 96 (2), pp. 503–512.

[7] Jones, W., and Navarro-Martinez, S., 2007, "Large eddy simulation of autoignition with a subgrid probability density function method", *Combust Flame*, Vol. 150 (3), pp. 170–187.

[8] Bulat, G., Jones, W., and Marquis, A., 2014, "NO and CO formation in an industrial gas-turbine combustion chamber using LES with the Eulerian sub-grid PDF method", *Combust Flame*, Vol. 161 (7), pp. 1804–1825.

[9] Hodzic, E., Jangi, M., Szasz, R.-Z., and Bai, X.-S., 2017, "Large eddy simulation of bluff body flames close to blow-off using an Eulerian stochastic field method", *Combust Flame*, Vol. 181, pp. 1–15.

[10] Tyliszczak, A., 2016, "High-order compact difference algorithm on half-staggered meshes for low Mach number flows", *Comput Fluids*, Vol. 127, pp. 131–145.

[11] Geurts, B., 2004, *Elements of Direct and Large-eddy Simulation*, R.T. Edwards.

[12] Vreman, A., 2004, "An eddy-viscosity subgrid-scale model for turbulent shear flow: Algebraic theory and applications", *Phys Fluids*, Vol. 16 (10), pp. 3670–3681.

[13] Tyliszczak, A., 2015, "LES–CMC study of an excited hydrogen flame", *Combust Flame*, Vol. 162 (10), pp. 3864–3883.

[14] Rosiak, A., and Tyliszczak, A., 2016, "LES-CMC simulations of a turbulent hydrogen jet in oxy-combustion regimes", *Int J Hydrog Energy*, Vol. 41 (22), pp. 9705–9717.

[15] Wawrzak, A., and Tyliszczak, A., 2019, "A spark ignition scenario in a temporally evolving mixing layer", *Combust Flame*, Vol. 209, pp. 353–356.

[16] Wawrzak, A., and Tyliszczak, A., 2020, "Study of a Flame Kernel Evolution in a Turbulent Mixing Layer Using LES with a Laminar Chemistry Model", *Flow Turbul Combust*, Vol. 105, pp. 807–835.

[17] Brown, P.N., and Hindmarsh, A.C., 1989, "Reduced Storage Matrix Methods in Stiff ODE Systems", *J Appl Math Comput*, Vol. 31, pp. 40–91.

[18] Mueller, M., Kim, T., Yetter, R., and Dryer, F., 1999, "Flow reactor studies and kinetic modeling of the H2/O2 reaction", *Int J Chem Kinet*, Vol. 31 (2), pp. 113–125.

[19] Kuban, L., Stempka, J., and Tyliszczak, A., 2021, "Numerical Analysis of the Combustion Dynamics of Passively Controlled Jets Issuing from Polygonal Nozzles", *Energies*, Vol. 14 (3), p. 554.